

# **A novel and inexpensive technique for creating superhydrophobic surfaces using Teflon and sandpaper**

**Michael A. Nilsson, Robert J. Daniello, Jonathan P. Rothstein\***

Department of Mechanical Engineering  
University of Massachusetts Amherst  
160 Governors Drive  
Amherst, MA 01003-2210

\*Corresponding author: rothstein@ecs.umass.edu

## **Abstract:**

Great efforts have been spent over the last decade developing hydrophobic surfaces exhibiting very large contact angles with water. Many of these methods require complex and expensive fabrication techniques. We demonstrate that sanding Teflon can produce superhydrophobic surfaces with advancing contact angles of up to  $151^\circ$  and contact angle hysteresis of less than  $4^\circ$ . Furthermore, we show that a wide range of both advancing contact angles and contact angle hysteresis can be achieved by varying the grit size of the sandpaper, allowing for future hysteresis and contact angle studies. Scanning Electron Microscopy (SEM) images of the roughened surfaces depict the range and amplitude of lengthscales imparted on the surface by the sandpaper, which leads to deeper understanding of the state of wetting on the surface.

**Subject Classification Numbers:** 68.08.Bc, 68.08.-p, 68.35.Ct, 47.55.dr, 47.55.np, **47.85.-g**, 68.35.Md, 68.37.-d, 62.10.+s, 47.55.D-, 68.37.Hk

**Submitted to:** Journal of Physics D: Applied Physics

## Text

A great deal of effort has been spent over the last decade developing hydrophobic surfaces exhibiting very large contact angles with water<sup>1-15</sup>. A number of strategies have been employed to increase the average contact angle between a substrate and water, including chemical modification of the substrate to lower the surface energy between the water and the surface<sup>1</sup>. However, it has been shown both theoretically<sup>6</sup> and experimentally with water<sup>10</sup> that chemical alteration of a smooth surface can only achieve advancing contact angles,  $\theta_A$ , with water up to about  $\theta \leq 130^\circ$ <sup>9</sup>. A surface is considered to be superhydrophobic if it has both a large advancing contact angle, greater than  $\theta_A > 150^\circ$ , and minimal contact angle hysteresis<sup>15</sup>. The contact angle hysteresis is defined as the difference between the advancing and receding,  $\theta_R$ , contact angles. Reducing contact angle hysteresis is widely accomplished in practice by introducing either random or precisely patterned surface roughness to a hydrophobic substrate.

These superhydrophobic surfaces were first inspired by the characteristic water repellency of the sacred lotus leaf<sup>16</sup>. Additionally, there are a number of other superhydrophobic surfaces found throughout nature in both the plant and insect world<sup>17</sup>. When properly designed, these bio-mimetic surfaces can reduce the contact angle hysteresis of water by maintaining an air-water interface above the depressions between the peaks of the surface roughness. Moreover, it has been shown that it is often advantageous to have multiple lengthscales of roughness in order to increase both advancing and receding contact angles while simultaneously minimizing hysteresis<sup>18</sup>.

Superhydrophobic surfaces have demonstrated the ability to be self-cleaning. As water droplets move along these surfaces, they roll, collecting dust and particulates from the surface<sup>19</sup>. Droplets move very easily along superhydrophobic surfaces because the drag force is proportional to the contact angle hysteresis,  $F_D \propto \cos(\theta_A - \theta_R)$ . Minimizing the hysteresis allows drops to be easily dislodged by even the smallest perturbations<sup>7, 14, 20, 21</sup>. The high level of water droplet mobility on superhydrophobic surfaces is desirable in many industrial applications. Some notable areas where the application of superhydrophobic

surfaces is emerging include automotive, transportation, communication hardware, marine technology, textiles, and biological applications. Specific examples of these applications being self-cleaning windows or antennas, stain-proof and water repellent clothing, and snow repellent satellite dishes <sup>3, 9, 12, 13, 22, 23</sup>.

These surfaces also facilitate the control and manipulation of individual drop-directed motion, allowing for the possible use of these surfaces in microfluidic applications.

The two major models to describe water contact angles on rough surfaces are the Cassie and the Wenzel model. In the Cassie state, an air-water interface is supported between the surface roughness <sup>24</sup>. This phenomena modifies the contact angle,  $\theta_c$ , such that

$$\cos(\theta_c) = \gamma(\cos(\theta) + 1) - 1. \quad (1)$$

Here  $\theta$  is the equilibrium contact angle between a smooth surface sample and the liquid as defined by Young's law, and  $\gamma$  is the area fraction of the solid-liquid interface. In order to maximize the equilibrium contact angle, the percent coverage of the air-water interface must similarly be maximized. It is also important to note that the shape and size of the surface protrusions affect the contact angle and resulting hysteresis <sup>11</sup>. At sufficiently large microfeature spacing and liquid pressures, the air-water interface can collapse, resulting in a fully wetted Wenzel state <sup>25</sup>. The equilibrium contact angle for the Wenzel state,  $\theta_w$ , is given by

$$\cos(\theta_w) = r \cos(\theta). \quad (2)$$

Here  $r$  is the ratio of the wetted area to the projected surface area. For a smooth surface,  $r = 1$ , and increases with increasing roughness. For a hydrophobic surface, the equilibrium angle will increase in the Wenzel state, however the contact angle hysteresis is also typically very large. This is due to the contact line being pinned at each wetted feature as it recedes <sup>26</sup>. Furthermore, it has been shown that even with proper spacing of surface features, that at a small scale the roughness cannot sufficiently "trap" air, and an increased hysteresis is experienced <sup>8</sup>. Therefore, true superhydrophobic surfaces therefore exist in the Cassie, not Wenzel state.

There are many methods by which roughness may be introduced to a material, including chemical or mechanical processes, oftentimes in concert with each other<sup>1, 7, 8, 10, 11, 14, 19-21, 26, 27</sup>. These methods generally necessitate extensive material or facility costs, however, there have been efforts made in minimizing these requirements<sup>4, 5</sup>. This letter focuses on the simple mechanical surface alteration of polytetrafluoroethylene (PTFE), commercially known as Teflon, renowned for its water-repellent properties. Biological, commercial and industrial applications comprise a few of Teflon's various uses. Teflon is naturally hydrophobic, featuring a smooth surface with contact angles,  $\theta_A / \theta_R$ , of  $128^\circ / 78^\circ$ , the average contact angle being  $103^\circ$ . The unaltered surface has large hysteresis,  $\theta_A - \theta_R = 50^\circ$ , restricting drop movement. Teflon's low coefficient of friction with many materials and consequently its "non-stick" properties are its primary appeal for its wide use in cookware. Teflon is also applied to fabrics (Goretex) and structural components (dome roofs) which take advantage of its water repellency.

This letter presents a simple and inexpensive method of creating a superhydrophobic surface, possessing a high advancing contact angle, and a hysteresis comparable to surfaces produced via more complicated and costly methods. The primary method used was simple sanding and subsequent cleaning of solid Teflon. We mounted each Teflon sample to pieces of aluminum using epoxy, in order to ensure a generally flat and secure Teflon surface. After letting the epoxy set, each sample was held stationary, and sanded by hand. Reasonable force is applied to impart a good representation of the grit size of the sand paper onto the Teflon. Sanding is performed in a random manner, as to show no preference in any particular direction. After approximately 20 seconds of sanding, the sanded surface is then cleaned with acetone briefly, then rinsed with reverse-osmosis deionized water, and dried with pressurized air. It is important to note that the final hydrophobic properties were not sensitive to additional sanding, excess pressure when sanding, or the use of a mechanical sander. The cost of a Teflon surface and sand paper is on the order of dollars, while more complicated methods can be on the order of hundreds to thousands of dollars for the materials and equipment required for production.

A range of commercial sand paper grit designations between 40-grit and 600-grit were used, with each sample being sanded by only one grit designation. Table 1 shows the common grit designation for the sandpaper used, the average particle size on the paper, and the average RMS roughness of the Teflon surface following sanding. Surface roughness measurements were taken using a Zygo 7300 optical profilometer, with each surface measured three times in three different locations over an area of 0.045 mm<sup>2</sup>. The resulting surface roughness imparted by the sanding exhibits a wide disparity between the various grit sizes. The smooth Teflon had the lowest average RMS roughness of 5.6 μm. As coarser sandpapers are used, the RMS roughness increased as is expected. As seen in equations (1) and (2), this increase in surface roughness is a mechanism by which contact angle can be increased.

The contact angle was measured photographically using an in-house constructed goniometer and is listed in Table 1 and presented graphically in Figure 1. Each contact angle measurement was taken three times, each in a different location on the Teflon surface. The volume of each drop was kept constant, and in each case the drop was well below a Bond number of one to ensure gravitational effects were negligible.

The Teflon prepared with the finest sandpaper, 600-grit, exhibited greater hysteresis than the smooth Teflon, as well as a larger advancing contact angle, suggesting that the added roughness exists primarily in the Wenzel state. As the grit size was increased from 600-grit to 360-grit, the advancing contact angle continued to increase with little change in the contact angle hysteresis. At a grit size of 320-grit, corresponding to a RMS roughness of 10μm, the advancing contact angle reached a maximum value of  $\theta_A = 151^\circ$  and the contact angle hysteresis showed a significant decrease. This data is suggestive of a transition from a mostly Wenzel to a mostly Cassie state of wetting. The contact angle hysteresis was further minimized as the grit size is increased from the 320-grit to the 180-grit. Of the surfaces with lower contact angle hysteresis, the 240-grit sanded Teflon had the least amount of hysteresis, 4°, which competes well with many of the published surface preparation techniques that possess similar hysteresis but are either much more expensive or require more complicated methods to produce<sup>9</sup>. As seen in Figure

1, two distinct regimes in the data become clearly apparent. The first at large sandpaper grits where the hysteresis remains fixed and advancing contact angle varies over a range of about  $30^\circ$ , and the second at lower sandpaper grits where the advancing contact angle is nearly constant at  $\theta_A \approx 150^\circ$  and the contact angle hysteresis varies over more than  $60^\circ$ . It is important to note that contact angle hysteresis is a key component when determining whether a droplet will move freely on a surface, or adhere<sup>1, 26, 27</sup>. The large variation of contact angle hysteresis in the second regime suggests that this surface preparation technique is well suited for systematically studying the effect of hysteresis on drop dynamics.

The advancing contact angle only marginally decreased as the grit size was increased from the 120-grit to the 40-grit, however, the contact angle hysteresis began to increase for grit designations smaller than 120-grit. The largest grit designation tested, 40-grit, still possessed a highly hydrophobic advancing contact angle, though their contact angle hysteresis approached that of smooth Teflon. Scanning electron microscopy (SEM) in Figure 2 shows that this deterioration of superhydrophobic character is likely caused by the large spacing between the surface features resulting from the large grit size and a suspected transition back to the Wenzel state from the Cassie state achieved for grits between 240- and 120-grit.

SEM images were taken of a subset of the surfaces listed in Table 1 and are shown in Figure 2. The Teflon surfaces were sputter-coated with gold and measurements were taken at 20kV. While the untreated Teflon is relatively smooth, sanding with the 600 grit sandpaper introduces surface roughness by coarsening the Teflon surface. While this roughness serves to increase the advancing contact angles, the valleys are not deep enough to maintain an air-water interface, giving further support to the hypothesized Wenzel state of wetting. This results in lower receding contact angles because the water is pinned to the surface along the receding contact, increasing the hysteresis substantially, as shown in Figure 1. As the sandpaper increases in grain size (or decreases in grit designations), the amplitude of the surface peaks and valleys increases, while the second level of roughness becomes more obvious on the Teflon substrate. This is shown with the 320-grit sanded Teflon with noticeably deeper depressions in

the surface, and furthermore with the 240-grit sanded Teflon. These deeper surface features and more pronounced secondary roughness likely allows for the formation of air-water interfaces typical of the Cassie state, resulting in even higher contact angles and reduced contact angle hysteresis. However, as the surface roughness increases even further, as seen with the 80-grit in Figure 2, some of the valleys and depressions become large, making the support of an air-water interface less likely, resulting in the gradual transition back into the Wenzel state. The effect of sanding other naturally hydrophobic surfaces will be investigated in the near future.

In this letter, we have shown that by sanding Teflon with various grits of sandpaper, it is straight forward to create surfaces with a wide range of hydrophobic properties. It is possible to create surfaces with an array of hydrophobic characteristics, from low contact angles and high hysteresis, to ones with very high contact angles and low hysteresis competitive with those produced by more expensive and complicated techniques. It is worthy to note that sanded Teflon surfaces possess relatively short regions of continuous air-water interfaces which are ideal for modifying the ease of drop motion on the surface.

### **Acknowledgments**

The authors acknowledge the Office of Naval Research for the support provided for this research under grant N00014-06-1-0497. The authors also thank Al Crosby for use of his Optical profilometer. Finally, the authors thank the UMASS MRSEC for use of its SEM.

## References

1. Chen, W. et al. Ultrahydrophobic and ultralyophobic surfaces: Some comments and examples. *Langmuir* 15, 3395-3399 (1999).
2. Duez, C., Ybert, C., Clanet, C. & Bocquet, L. Making a splash with water repellency. *Nature Physics* 3, 180-183 (2007).
3. Daniello, R. & Rothstein, J. P. Turbulent drag reduction using ultrahydrophobic surfaces. *Physics of Fluids In Press* (2009).
4. Gao, L. C. & McCarthy, T. J. An "artificial lotus leaf" prepared using a 1945 patent and a commercial textile. *Abstracts of Papers of the American Chemical Society* 231, - (2006).
5. Gao, L. C. & McCarthy, T. J. A commercially available perfectly hydrophobic material ( $\theta(A)/\theta(R)=180$  degrees/180 degrees). *Langmuir* 23, 9125-9127 (2007).
6. Girifalco, L. A. & Good, R. J. A Theory for the Estimation of Surface and Interfacial Energies .1. Derivation and Application to Interfacial Tension. *Journal of Physical Chemistry* 61, 904-909 (1957).
7. Kim, J. W. & Kim, C. J. Nanostructured surfaces for dramatic reduction of flow resistance in droplet-based microfluidics. *Fifteenth Ieee International Conference on Micro Electro Mechanical Systems, Technical Digest*, 479-482 737 (2002).
8. Miwa, M., Nakajima, A., Fujishima, A., Hashimoto, K. & Watanabe, T. Effects of the surface roughness on sliding angles of water droplets on superhydrophobic surfaces. *Langmuir* 16, 5754-5760 (2000).
9. Nakajima, A., Hashimoto, K. & Watanabe, T. Recent studies on super-hydrophobic films. *Monatshefte Fur Chemie* 132, 31-41 (2001).
10. Nishino, T., Meguro, M., Nakamae, K., Matsushita, M. & Ueda, Y. The lowest surface free energy based on -CF<sub>3</sub> alignment. *Langmuir* 15, 4321-4323 (1999).
11. Oner, D. & McCarthy, T. J. Ultrahydrophobic surfaces. Effects of topography length scales on wettability. *Langmuir* 16, 7777-7782 (2000).
12. Ou, J. & Rothstein, J. P. Direct velocity measurements of the flow past drag-reducing ultrahydrophobic surfaces. *Physics of Fluids* 17, - (2005).
13. Saito, H., Takai, K. & Yamauchi, G. Water- and ice-repellent coatings. *Jocca-Surface Coatings International* 80, 168-& (1997).
14. Shastry, A., Case, M. J. & Bohringer, K. F. Directing droplets using microstructured surfaces. *Langmuir* 22, 6161-6167 (2006).
15. Tadanaga, K., Morinaga, J., Matsuda, A. & Minami, T. Superhydrophobic-superhydrophilic micropatterning on flowerlike alumina coating film by the sol-gel method. *Chemistry of Materials* 12, 590-+ (2000).
16. Neinhuis, C. & Barthlott, W. Characterization and distribution of water-repellent, self-cleaning plant surfaces. *Annals of Botany* 79, 667-677 (1997).
17. Bush, J. W. M., Hu, D. L. & Prakashc, M. The integument of water-walking arthropods: Form and function. *Advances in Insect Physiology: Insect Mechanics and Control* 34, 117-192 (2007).
18. Gao, L. C. & McCarthy, T. J. The "lotus effect" explained: Two reasons why two length scales of topography are important. *Langmuir* 22, 2966-2967 (2006).
19. Mahadevan, L. & Pomeau, Y. Rolling droplets. *Physics of Fluids* 11, 2449-2453 (1999).
20. Bico, J., Marzolin, C. & Quere, D. Pearl drops. *Europhysics Letters* 47, 220-226 (1999).
21. Sakai, M. et al. Direct observation of internal fluidity in a water droplet during sliding on hydrophobic surfaces. *Langmuir* 22, 4906-4909 (2006).
22. Kissa, E. (ed.) *Repellent Finishes* (Marcel and Dekker Inc., New York, 1984).

23. Schakenraad, J. M., Stokroos, I., Bartels, H. & Busscher, H. J. Patency of Small Caliber, Superhydrophobic E-Ptfe Vascular Grafts - a Pilot-Study in the Rabbit Carotid-Artery. *Cells and Materials* 2, 193-199 (1992).
24. Cassie, A. B. D. & Baxter, S. Wettability of porous surfaces. *Transactions of the Faraday Society* 40, 0546-0550 (1944).
25. Wenzel, R. N. Resistance of solid surfaces to wetting by water. *Industrial and Engineering Chemistry* 28, 988-994 (1936).
26. Lafuma, A. & Quere, D. Superhydrophobic states. *Nature Materials* 2, 457-460 (2003).
27. Quere, D., Azzopardi, M. J. & Delattre, L. Drops at rest on a tilted plane. *Langmuir* 14, 2213-2216 (1998).

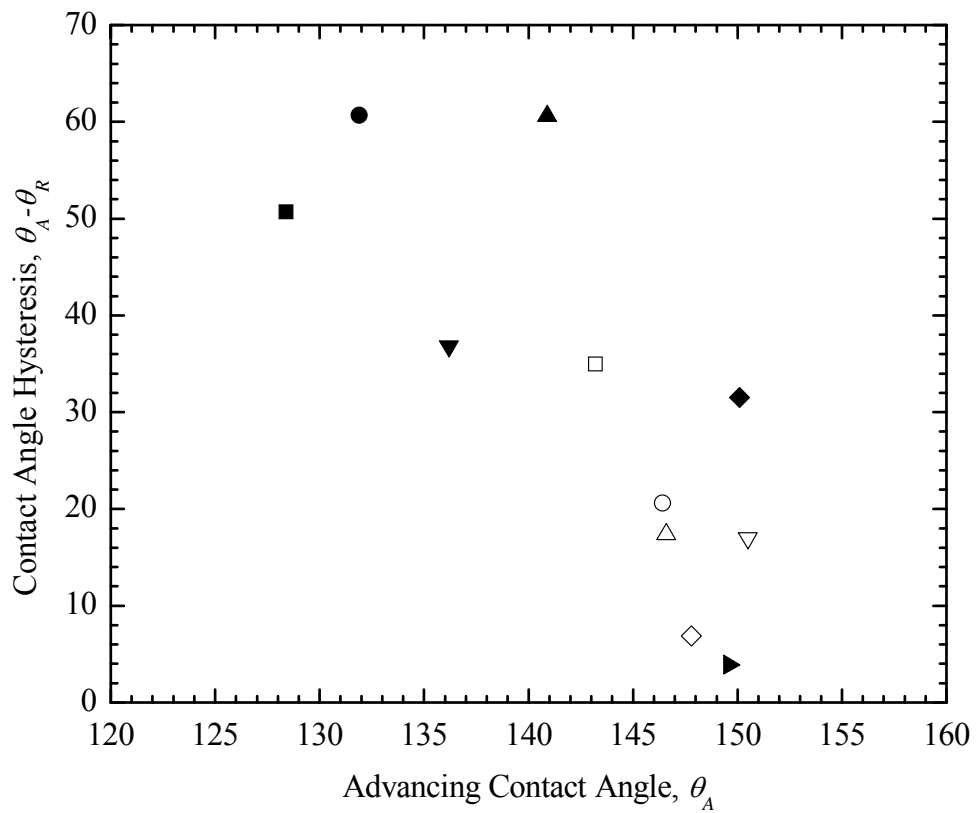


**Figure 1:** Hysteresis as a function of advancing contact angle for smooth ■ Teflon, as well as a series of Teflon surfaces, sanded with sandpaper of grit designation ● 600, ▲ 400, ▼ 360, ◆ 320, ▶ 240, ◇ 180, ▽ 120, △ 80, ○ 60, and □ 40.

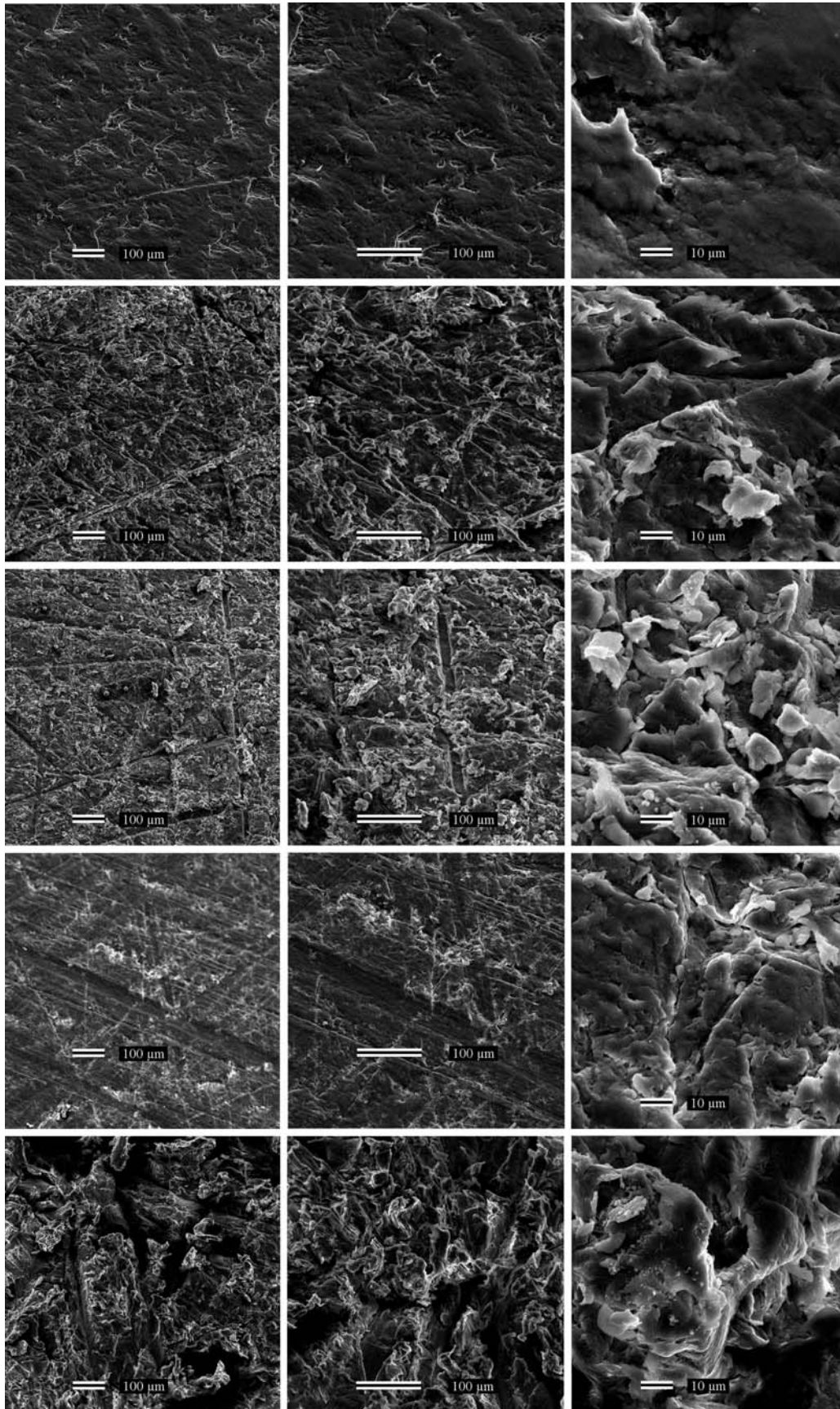


**Figure 2:** SEM images of a series of Teflon surfaces sanded with sandpaper of various grit designations. The magnification is increased left to right from 100x to 200x to 1000x. The grit designation of the sand paper is decreased top to bottom from smooth (unsanded) to 600-grit, 320-grit, 240-grit, and 80-grit.

**Table 1:** Characterization of both the sandpaper used and the resulting surface roughness and wetting properties of water and the sanded Teflon surfaces.

<b>Grit designation</b>	<b>Mean Particle Diameter (<math>\mu\text{m}</math>)</b>	<b>RMS Roughness Teflon (<math>\mu\text{m}</math>)</b>	<b>Contact Angle (<math>\theta_A / \theta_R</math>)</b>
Smooth	---	5.6	128°/78°
600	25.8	7.6	132°/71°
400	35.0	4.6	140°/80°
360	40.5	5.5	136°/99°
320	46.2	10.9	150°/119°
240	58.5	13.7	150°/146°
180	82	15.4	148°/141°
120	125	16.3	151°/134°
80	201	14.5	146°/129°
60	269	18.2	146°/125°
40	425	17.5	143°/108°